

Biomedical Evaluation of Biosynthesized FeO:CuO Ncs by Nigella Sativa Seeds Extract Against Breast Cancer Cell Line, and Bacterial Strains

Thaer A. Mezher¹, Abdullah M. Ali², Ahmed N. Abd³

^{1,2}Department of Physics, College of Education for Pure Science, Tikrit University, Iraq

³Department of Physics, College of Science, Mustansiriyah University, Iraq.

E-mail: amed_naji_abd@yahoo.com

Abstract

Using an economical, low-cost and safe method, iron oxide nanoparticles and copper oxide nanoparticles were prepared in a very short time using green synthesis technology and Nigella sativa seed extract, which is a reducing and covering agent at the same time. The prepared particles were identified through different techniques, as the results of X-ray diffraction (XRD) confirmed the composition of the two materials, the visible-ultraviolet spectrometer showed the presence of two absorption peaks in the infrared region and in the ultraviolet region, and the shape and size of the particles were determined by transmission electron microscopy. (TEM) It was spherical in shape and size ranged between 5 - 30 nm. The antibacterial activity was studied as well as the activity of the prepared material was also studied in the treatment of human breast cancer line MCF-7, where it was shown that the prepared material is well active to work in anti-cancer applications.

Keywords: Green synthesis, Nigella Sativa, FeO:CuO Nanocomposites, anticancer antibacterial activity

1. Introduction

In the rapidly developing field of nanotechnology, which provides opportunities for sustainable development at the atomic and nanoscale levels, nanoparticles are the most important structural masses there are. The present state of technological development necessitates the production of smaller and more miniature goods that consume less energy to run, require fewer resources to produce, and have the capacity to be recycled. Nanoparticles play an important role in a number of different scientific disciplines, including the delivery of medicines, the diagnosis of diseases, and the addition of ingredients to food [1,2]. Nanoparticles made of metal have emerged as the most important class of all the nanoparticles currently in existence. They are uncommon in nature as a result of the high surface to volume ratio that they possess. They create a link between the structure of atoms or molecules and the composition of the substance as a whole. Approaches that start at the bottom and work their way up are both used in the process of creating nanoparticles. Research into the characteristics of iron oxide nanoparticles is not given as much attention as research into the properties of gold and silver nanoparticles. This is because iron oxide nanoparticles have a high rate of oxidation. Because of their magnetic properties, nanoparticles of iron oxide could theoretically play an extremely important role. It can be used for a variety of purposes, including biosensing, the remediation of wastewater, the removal of heavy metals through

adsorption, and the manufacture of medicinal products. Copper oxide (CuO), a P-type semiconductor with a band gap ranging from 1.21 to 1.51 eV, is considered to be one of the more desirable oxides. Oxides of metals are the most adaptable category of materials because they exhibit properties that are relevant to all subfields of chemistry and physics. Copper oxide semiconductors have a number of advantageous qualities, including high levels of optical absorption, non-toxicity, and low manufacturing costs. In addition, there are fresh opportunities to investigate the bactericidal effects of novel nanomaterials that contain metals known for the putative bioactivities they exhibit. It is possible to produce metallic nanoparticles in large quantities using chemical (co-precipitation, chemical reduction, etc.) and physical (sol-gel, hydrothermal, ultrasonic bombardment, etc.) processes [3-5], but these procedures are expensive, time-consuming, toxic to living cells, and hazardous to the environment. To address the problems with traditional physical and chemical procedures, new techniques have been developed that leverage biological sources such microbes, microbial extracts/products, and plant extracts have been developed to address the problems caused on by traditional physical and chemical approaches [6-8]. Researchers are still working to develop simple, reliable, and effective green chemical methods to produce nanomaterials. Many organisms operate as safe, environmentally acceptable, and lengthy precursors to create stable, well-functionalized nanoparticles. Bacteria, actinomycetes, fungi, yeast,

viruses, etc. may be among these [9,10]. In this research, two types of metal oxides were prepared, nano-iron oxide and nano-copper oxide, by the green plant synthesis method, using *Nigella Sativa* seeds extract, and studying the properties of their nanocomposites (NCs), showing its biological effectiveness for different types of bacteria and breast cancer line MCF-7.

2. Materials and Methods

Nanoparticles of iron oxide and copper oxide were prepared by the plant green synthesis technique. The preparation process goes through several stages:

1) The stage of preparation of the plant extract: The seeds of the black seed plant were obtained from the local market in Baghdad, Fig (1-left) and the seeds were washed with water well to get rid of the dust attached to them, after which they were dried and ground using a crusher until we get the seed powder. 1 gm of the powder is dissolved in 100 ml of distilled water at a temperature of $50^{\circ}\text{C} \pm 10$ for half an hour using a heated magnetic stirrer, after that the solution is well filtered by filter paper and the plant extract is kept in the refrigerator to be used at a later time when needed

2) The stage of preparing the iron salts solution: we take 4.04 gm of iron nitrate $\text{Fe}(\text{NO}_3)_3 \cdot 9\text{H}_2\text{O}$ (1M) provided by (General Drug House - India, Purity 99.5%), which is completely dissolved in 100 mL of distilled water at room temperature

3) The stage of preparing the copper salts solution: We take 2.41 gm of copper nitrate $\text{Cu}(\text{NO}_3)_2 \cdot 3\text{H}_2\text{O}$ (1M) provided by (General Drug House - India, Purity 99.5%), which is completely dissolved in 100 ml of distilled water at room temperature

4) Iron oxide nanoparticles formation stage: 10 ml of

plant extract solution is added to 100 ml of dissolved iron salts solution gradually at a temperature of 60°C . and the addition process stops when the color change process of the solution and its acquisition of color is observed red, which is evidence of the formation of iron oxide nanoparticles.

5) The stage of formation of copper oxide nanoparticles: which is the last stage of the preparation stages in which 5 ml of a plant extract solution is added to 100 ml of a solution of dissolved copper salts gradually at a temperature of 60°C , and the addition process stops when the color change process of the solution and its acquisition of color is observed green, which is evidence of the formation of copper oxide nanoparticles.

6) In the last step, the nanocomposite is obtained by mixing equal amounts of each of the solutions containing iron oxide and copper oxide. 3 ml of each of the two solutions is mixed in a tube and used in diagnostic techniques and in medical application in antibacterial and anticancer activity.

7) The pH value was fixed at 7 during the experimental period

Drop casting technique Fig(1-right) was used to precipitate a solution of iron oxide nanoparticles and copper oxide nanoparticles on glass substrates to perform the structural characterization process using an XRD 2700AB diffractometer (HAOYUAN, Zhejiang, China). As for the vibrational characteristics, Fourier Transformation Infrared spectroscopy (FTIR) (SHIMADZU - 8400 S) was used. and morphological characteristics, a diagnosis was made Transmission Electron Microscopy (TEM) Philips em 208s 100 Kv. and the optical properties, a UV-Vis LAMBDA 365 spectrophotometer (PerkinElmer, Waltham, MA, USA) was tested.



Figure:1 Left : *Nigella Sativa* plant parts, Right : Drop casting technique

The MCF-7 line of human breast cancer cells was employed to assess the cytotoxic activity of $\text{FeO}:\text{CuO}$ NCs. The MCF-7 cells were obtained from Malaya University's Faculty of Medicine's Pharmacology Department in Kuala Lumpur, Malaysia, and were derived from Dr. Ahmad Fadhil (Al-Nahrin University, Iraq). The cell suspension was spread in a humidified cell culture that contained 5% CO_2 , 21% O_2 , and 37°C . All cell lines were

maintained in RPMI 1640 media supplemented with 10% heat-inactivated. Each experiment was carried out in triplicate using data from three separate experiments.

3. Result and Discussion

X-ray diffraction was utilized so that the structural qualities of thin layers could be investigated. The thin films were obtained by drop casting of a

nanoparticles solution consisting of nanoparticles of iron oxide and copper oxide. These nanoparticles were deposited on glass substrates heated to sixty degrees in order to obtain a homogeneous thin film consisting of distributed nanoparticles. Figure (2) shows the XRD spectrum of the nanostructure formation of nanoparticles of iron oxide and copper oxide Nano synthesized by ferrous nitrate and copper nitrate solutions, respectively, with Nigella sativa seed extract. The Bragg peak was observed at specific angles and levels that it is related to copper oxide and its phases, while other diffraction peaks confirmed that it is due to iron oxide and its different phases. To show the accuracy of the results we

obtained, we compare the results with a JCDPS cards. Through the Debye-Scherrer relation, the crystallite size Dave is calculated according to the relation:[11]

$$D_{avg} = k \cdot \lambda / (\beta \cos \theta) \quad (1)$$

where $\lambda = (1.5406 \text{ \AA})$, k is the shape factor, and θ is the diffraction angle, β is the full width at half maximum (measured in degrees). Calculating the strain value and dislocating density value may be done using equations 2 and 3 and listed in Table 1.[12].

$$\delta = (D_{avg})^{-2} \quad (2)$$

$$\eta = (\cot \theta \times \beta) / 4 \quad (3)$$

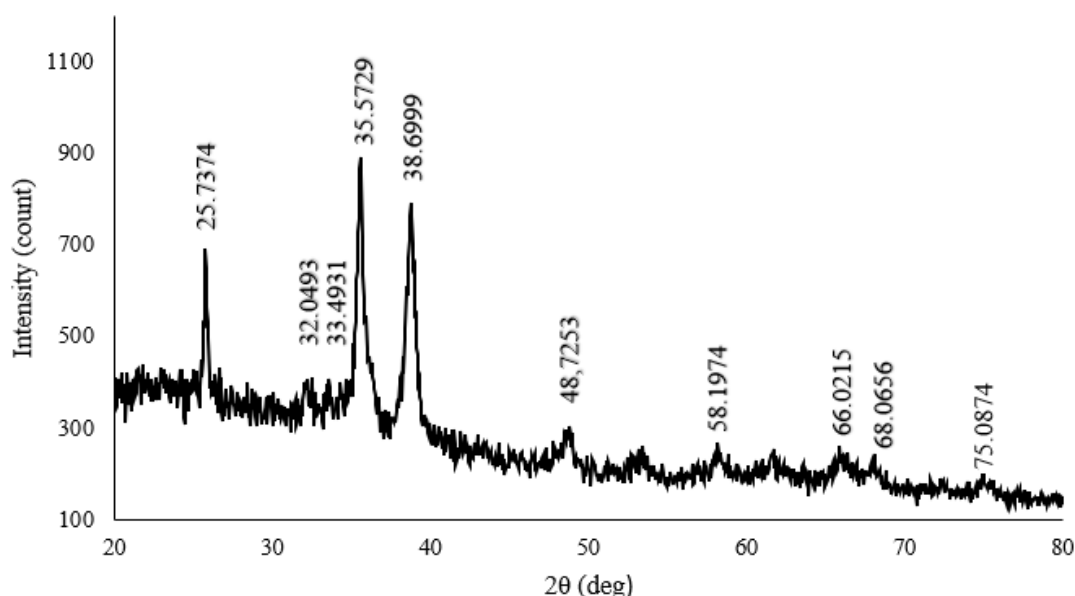


Figure 2: X-ray diffraction of FeO:CuO NCs layers

| Table 1: Structural Parameters FeO:CuO NCs prepared by green synthesis | | | | | | | | | |
|--|----------------------------------|------------|-----|--------|-------------|------------|---------------|-------------------|-------------|
| Peak position | phases | Peak JCPDS | hkl | FWHM | d (Å) JCPDS | Gsize (nm) | Strain x10e-4 | dislocation 10E14 | JCPDS |
| 25.7373 | Fe ₂ O ₃ | 26.1 | 211 | 0.1968 | 2.8420 | 41.188 | 8.41253 | 5.8945044 | 00-039-1364 |
| 32.0493 | ε-Fe ₂ O ₃ | 31.8 | 003 | 0.3936 | 2.7764 | 20.891 | 16.5854 | 22.911155 | 00-016-0653 |
| 33.4931 | β-Fe ₂ O ₃ | 33.8161 | 116 | 0.2952 | 2.6485 | 27.960 | 12.3925 | 12.791370 | 00-040-1139 |
| 35.5729 | CuO | 35.5431 | 111 | 0.2952 | 2.5236 | 28.120 | 12.3221 | 12.646323 | 00-048-1548 |
| 38.6999 | CuO | 38.7081 | 111 | 0.2460 | 2.3242 | 34.058 | 10.1737 | 8.6209131 | 00-048-1548 |
| 48.7253 | CuO | 48.763 | 202 | 0.4920 | 1.8600 | 17.644 | 19.6377 | 32.119985 | 00-005-0661 |
| 58.1974 | Cu ₄ O ₃ | 58.3553 | 224 | 0.5904 | 1.5803 | 15.336 | 22.5931 | 42.515373 | 00-003-0879 |
| 66.0215 | β-Fe ₂ O ₃ | 65.918 | 622 | 0.9840 | 1.4612 | 9.5929 | 36.1203 | 108.66717 | 00-039-0238 |
| 68.0656 | CuO | 68.140 | 220 | 0.5904 | 1.3320 | 16.180 | 21.4146 | 38.195773 | 00-005-0661 |
| 75.0874 | CuO | 74.9461 | 202 | 1.2 | 1.2661 | 8.3249 | 41.6216 | 144.28839 | 00-044-0706 |

Figure 3 shows the FTIR spectra of FeO:CuO NCs, which contained several distinct absorption peaks. The FeO:CuO stretching vibration mode is thought to be responsible for the large absorption band in the (500-800) cm⁻¹ range. The band at 3456 cm⁻¹ is attributed to the band O-H stretching vibrations, according to this figure, whereas the band around 1636 cm⁻¹ is assigned to the C=C bending vibrations mode. They demonstrate that the sample has a minor quantity of absorbed water in it. The bands at 1079, 1134 and 1197 cm⁻¹ denotes the existence of C-O in the precursor, but the band at 1384 cm⁻¹ is mainly caused by the banded vibration of ionic C-H.

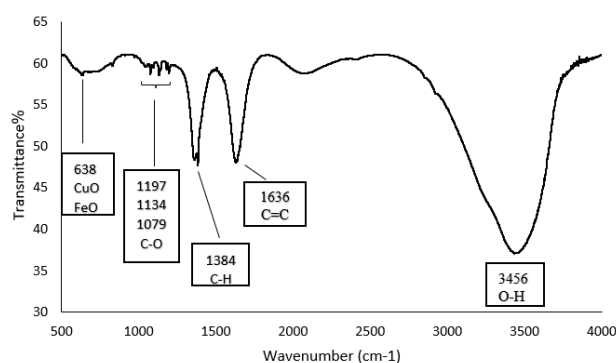


Figure 3: FTIR spectrum of FeO:CuO NCs

In Figure 4, a TEM image of FeO:CuO NCs is shown. The picture made it very clear that the green synthesis was what produced the FeO:CuO NCs. It has been demonstrated that spherical and semispherical nanoparticles come in two distinct varieties. The first of them has huge dimensions and is referred to be a huge structure. The fact that these particles are proteins makes them unique to the method of synthesis utilized by green plants. The FeO:CuO NCs, which belong to the second category of nanoparticles, are distinguished by their dark black hue and sizes of between 5 and 30 nm

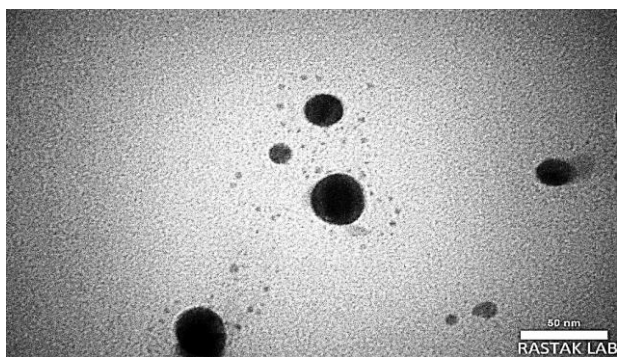


Figure 4: TEM image of FeO:CuO NCs

The UV-Vis spectra of FeO:CuO NCs that were synthesized by using Nigella sativa seed extract are shown in Figure 5. The rapid transformation of the ferrous nitrate solution into a scarlet color after the plant extract was gradually added to it. We also notice the transition to the green color of the copper nitrate solution when Adding the plant extract to it

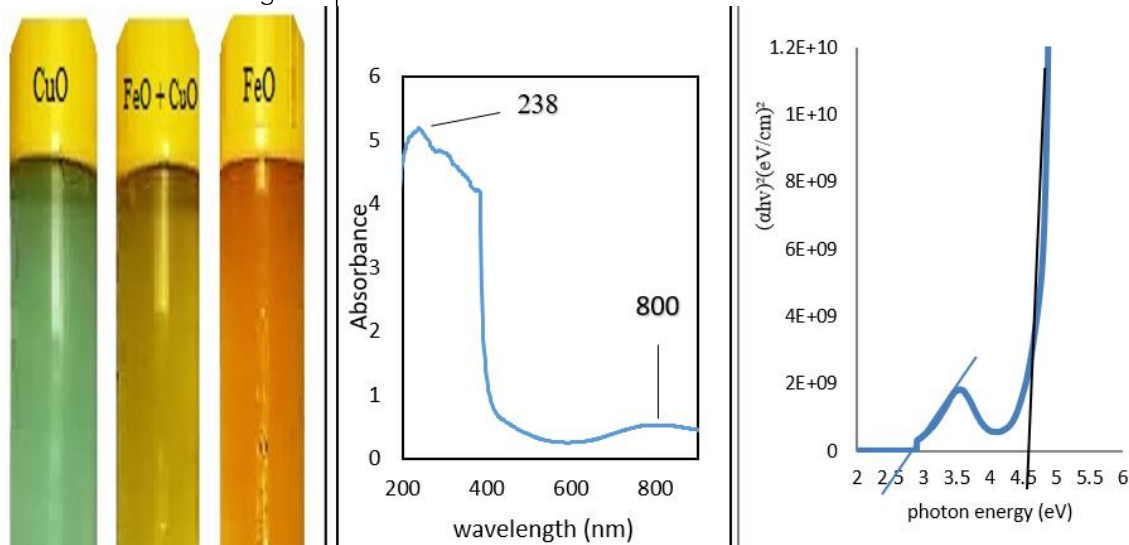


Figure 5: Left, shows the Color changing and formation of FeO:CuO NPs , Middle: shows the optical absorbance spectrum , Right: shows the optical energy bandgaps

Now, the medical industry has begun to investigate one of nanotechnology's most advantageous uses. Antibiotics, which only kill a certain subset of pathogens, have a far less potential to eliminate a much larger range of infectious illnesses than nanoparticles. In order to prevent themselves from being wiped out by antibiotics, bacteria have developed a wide range of resistance mechanisms throughout the years. Contrary to popular belief, the biofilm state does not directly impart antibiotic resistance; rather, antibiotic resistance that is

and when mixing the two solutions to form the nanocomposite, the resulting solution is greenish-red in color (Fig. 6 left). On the other hand, the generated FeO:CuO NCs show two distinct absorption regions, the first peak is located at 800 nm within the infrared region, then the absorption gradually decreases as it progresses towards the visible light region until it reaches its lowest level. As for the characteristic peak of the second absorption region, it is located in the 238 nm range in the ultraviolet range which is due to the surface plasmon resonance for CuO NPs [13], By applying the following formula to a tauc plot:[14] to calculate the optical energy gap of FeO:CuO NCs

$$\alpha h \nu = \beta (h\nu - E_{gopt}) n \dots\dots (4)$$

Where E_g is the optical energy gap, and n represents the number of transitions ($n = 0.5$). The absorption coefficient, plank constant, transition frequency, and other constants are denoted as, β , h , and ν respectively. The measurement was made by extrapolating the linear curve section VS. the photon energy from the square plot $(\alpha h\nu)^2$ toward the photon energy. FeO:CuO NCs thin film's energy gaps are determined to be 2.7 and 4.6 eV., (Fig. 6 Right) the values for the band gap increased. This behavior of Fermi fission indicates to the nanosituation, and an expansion of the permissible states brought on by an increase in charge carrier concentrations may lead to the development of two energy gaps. [15]

acquired genetically does. Bacteria may be able to get beyond the defense systems that stop them from responding to traditional antibiotics since they haven't before encountered nanoparticles. The ability to attack bacterial biofilms is another thing they have. [16]

The efficacy of synthesized FeO NPs to stop the development of pathogens (Gram +ve and Gram-ve bacteria) was examined using the agar well diffusion technique. The finding shows that the NPs have antibacterial and antifungal qualities..

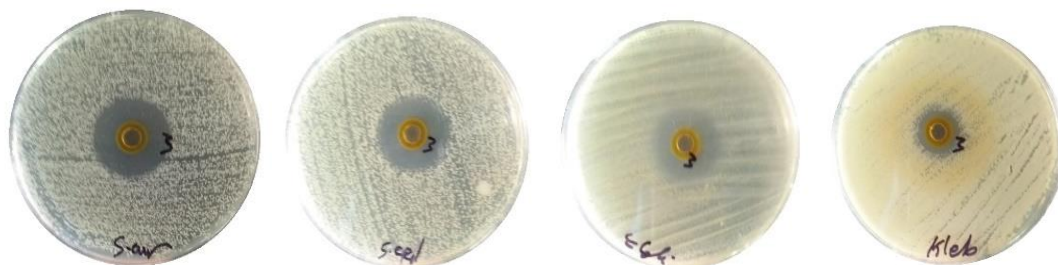


Figure 6: Biological activity of different types of bacteria

Figure 6 presents a visual representation of the influences that FeO:CuO NCs have on the biological activity of four distinct types of microorganisms. The green synthesis technique along with *Nigella sativa* seed extract were utilized during the production of these NCs. (*E. coli*, *Klebsiella* spp., *S. aureus*, and *S. epidermidis*). In Table 2, the inhibitory diameter was displayed in a manner that was both understandable and listed in Table 2

| Table 2: The bacterial inhibiting zone that occurs when FeO:CuO NCs are present. | | | | |
|--|------------------|-----------------------|----------------|----------------------|
| Bacteria | <i>S. aureus</i> | <i>S. epidermidis</i> | <i>E. coli</i> | <i>Klebsiella</i> sp |
| Inhibition zone (mm) | 26 | 25 | 22 | 18 |

Assays of cell viability not only report on living cells, but also provide a secondary indication of toxicity. (decrease in cell viability). In order to achieve this aim, the characteristics of a suitable unaltered cell sample are evaluated and contrasted with those of a substance-treated cell sample. This technique is frequently utilized in the screening of novel drugs, substances, and compounds for the time- and dose-dependent impacts they have on the viability of cells. For instance, it is necessary if an examination of a biological process involves the utilization of substances that disrupt the process. (e.g. inhibitors). It is necessary to identify a dosage that, while producing the intended inhibitory effect, does not cause any toxicity. Another illustration of this would be the utilization of cell viability studies in order to establish the quantity of anti-cancer medication necessary to eradicate cancerous cells. The IC₅₀ value is a measurement that is frequently the outcome of such fundamental toxicological studies. (Inhibitory concentration 50). This term refers to the amount of drug that must be administered in order to achieve (50%) of the maximal inhibitory effect, or in this instance (50%) cell viability. (Fig.7). Also, the figure refers to the second reason for conducting measurements of cell viability is to compare the results of other cellular assays to the cell population or viability of the sample. In order to correct for toxicity and growth effects produced by test substances as well as differences in seeding, a viability normalization that is performed in multiplex with a functional assay is extremely helpful. This is especially significant when it comes to testing for cell death because there is a significant difference between determining that 10 cells out of 20 are dead and determining that 10 cells out of 1000 exhibit

signs of cell death. Therefore, in order to evaluate the toxicity of the experimental conditions, it is definitely necessary to acquire living cells in addition to dead cells. This is a prerequisite. We also note that the inhibition rate is very high for the mixture of iron and copper oxides, estimated at 64%. This may be attributed to the size of the small particles and their high concentration of charge carriers

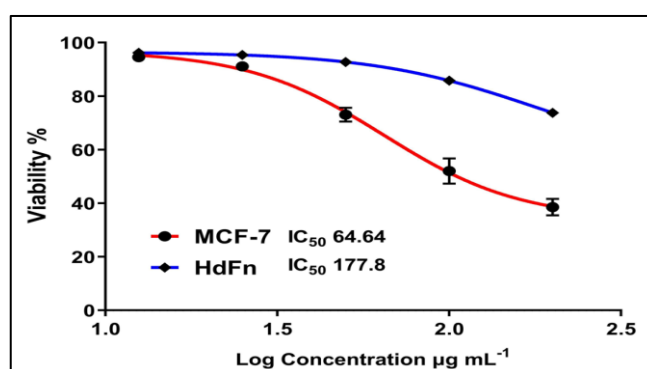


Figure 7: MTT assay chart gives the relative cell viability of breast cancer vs log concentration.

4. Conclusion

Identified biological components in *Nigella sativa* seed extract to produce iron oxide: copper oxide nanoparticles were used for the purposes of this investigation. The manufactured nanoparticles were largely spherical in shape, and had an average diameter of between 5 and 30 nm. FeO and CuO nanoparticles (FeO:CuO) NCs were produced during the fabrication process. The synthesized nanoparticles showed good antibacterial activity for a wide range of Gram-positive and Gram-negative bacterial strains. and against breast cancer cell line. The prepared nanoparticles are well suited for use in biological applications because they are of low toxicity due to the reduced use of harmful chemicals compared to antibiotics produced through chemical synthesis, which have significantly harmful effects.

References

- Chaudhary, A., Kumar, N., Kumar, R., & Salar, R. K. (2019). Antimicrobial activity of zinc oxide nanoparticles synthesized from Aloe vera peel extract. *SN Applied Sciences*, 1, 1-9.
- [Abd, A. N., Ali, R. S., & Hussein, A. A. (2016). Fabrication And Characterization Of Heterojunction Nickel Oxide Nanoparticles/Silicon. *Journal of Multidisciplinary Engineering Science Studies*, 2(4).
- Tesh, S. J., & Scott, T. B. (2014). Nanocomposites for

water remediation: A review. *Advanced Materials*, 26(35), 6056-6068.

Nadagouda, M. N., Hoag, G., Collins, J., & Varma, R. S. (2009). Green synthesis of Au nanostructures at room temperature using biodegradable plant surfactants. *Crystal Growth & Design*, 9(11), 4979-4983

Hassoni, M. H., Aziz, W. J., Abd, A. N., & Habubi, N. F. (2019). Invention and description of p-CuO/n-Si (200°C) Heterojunction for Photodiode Applications. *Journal of Global Pharma Technology*, 11(02), 601-606.

Sherwood, J., Xu, Y., Lovas, K., Qin, Y., & Bao, Y. (2017). Surface functionalization of dopamine coated iron oxide nanoparticles for various surface functionalities. *Journal of Magnetism and Magnetic Materials*, 427, 220-224.

Joerger, R., Klaus, T., & Granqvist, C. G. (2000). Biologically produced silver-carbon composite materials for optically functional thin-film coatings. *Advanced Materials*, 12(6), 407-409.

[8] Logeswari, P., Silambarasan, S., & Abraham, J. (2015). Synthesis of silver nanoparticles using plants extract and analysis of their antimicrobial property. *Journal of Saudi Chemical Society*, 19(3), 311-317.

Mandal, D., Bolander, M. E., Mukhopadhyay, D., Sarkar, G., & Mukherjee, P. (2006). The use of microorganisms for the formation of metal nanoparticles and their application. *Applied microbiology and biotechnology*, 69, 485-492.

Jebali, A., Ramezani, F., & Kazemi, B. (2011). Biosynthesis of silver nanoparticles by *Geotricum* sp. *Journal of Cluster Science*, 22, 225-232.

Abd, A. N., Abd Al Hussan, S. M., & Latif, D. M. (2020). Green synthesis and characterization of the prepared aloe vera plant extract thin film in a simple chemical method. *strain*, 10(4).

Abd Al Hussan, S. M., Bakr, N. A., & Abd, A. N. (2020, November). Improve the Performance of Porous Silicon for solar application by the embedding of Lithium Oxide nanoparticle. In *IOP Conference Series: Materials Science and Engineering* (Vol. 928, No. 7, p. 072142). IOP Publishing.

Mali, S. C., Raj, S., & Trivedi, R. (2019). Biosynthesis of copper oxide nanoparticles using *Encostemma axillare* (Lam.) leaf extract. *Biochemistry and biophysics reports*, 20, 100699.

Abd, A. N., Habubi, N. F., Reshak, A. H., & Mansour, H. L. (2018). Enhancing the Electrical Properties of Porous Silicon Photodetector by Depositing MWCNTs. *International Journal of Nanoelectronics & Materials*, 11(3).

Shakir, I. A., Ali, R. S., Almosawi, Z. A., and Abd, A. N. (2022). Study of Eco-accommodating and Reliable method to Synthesis ZnO NPs by Hibiscus sabdariffa plant and their Bio-applications. *International Journal of Scientific and Academic Research*, 2(6), 19-27.

Makabenta, J. M. V., Nabawy, A., Li, C. H., Schmidt-Malan, S., Patel, R., and Rotello, V. M. (2021).

Nanomaterial-based therapeutics for antibiotic-resistant bacterial infections. *Nature Reviews Microbiology*, 19(1), 23-36.